

Lepton Flavor Violation in τ decays at BABAR ^a

Swagato Banerjee ^b

University of Victoria, British Columbia, V8W 3P6 Canada.

E-mail: swaban@slac.stanford.edu

Abstract. Searches for lepton flavor violating $\tau \rightarrow \ell\gamma$, $\tau \rightarrow \ell\ell\ell$ and $\tau \rightarrow \ell hh$ decays at the BABAR experiment are presented. Upper limits on the branching ratios are obtained at the level of $O(10^{-7})$ at 90% confidence level.

1 Introduction

Lepton flavor violating (LFV) processes such as the neutrinoless decay of the τ lepton have long been identified as unambiguous signatures of new physics, because no known fundamental local gauge symmetry forbids such a decay. While forbidden in the Standard Model (SM) because of vanishing neutrino mass in the three lepton generations, extensions to include current knowledge of neutrino mass and mixing imply $\mathcal{B}(\tau \rightarrow \mu\gamma) \sim \mathcal{O}(10^{-54})$ [1], which is many orders of magnitude below the experimental sensitivity. However, many new theories, as tabulated below, allow for LFV decays: $\tau \rightarrow \ell\gamma$, $\tau \rightarrow \ell\ell\ell$, $\tau \rightarrow \ell hh$ (where $\ell = e, \mu$; $h = \pi, K$) up to their existing experimental bounds $\sim \mathcal{O}(10^{-7})$:

	$\mathcal{B}(\tau \rightarrow \ell\gamma)$	$\mathcal{B}(\tau \rightarrow \ell\ell\ell)$
mSUGRA + seesaw [2, 3]	10^{-7}	10^{-9}
SUSY + SO(10) [4, 5]	10^{-8}	10^{-10}
SM + seesaw [6]	10^{-9}	10^{-10}
Non-Universal Z' [7]	10^{-9}	10^{-8}
SUSY + Higgs [8, 9]	10^{-10}	10^{-7}

Feynman diagrams for $\tau \rightarrow \mu\gamma$ and $\tau \rightarrow \mu\mu\mu$ decays via s-neutrino mixing in minimal supergravity model with heavy ν_R (seesaw mechanism) and via neutral Higgs exchange in supersymmetric model are shown in Figure 1, respectively.

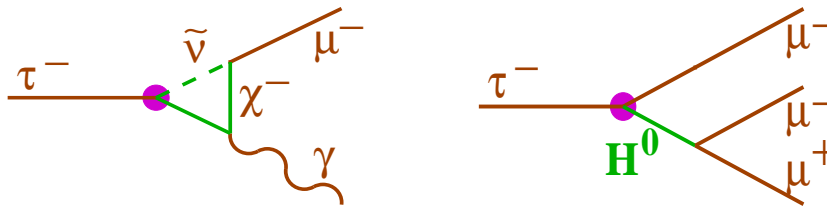


Figure 1: Illustrative scenarios for $\tau \rightarrow \mu\gamma$ (left) and $\tau \rightarrow \mu\mu\mu$ (right).

^aTo appear in the proceedings of XII Lomonosov Conference on Elementary Particle Physics, Moscow, Russia (25 - 31 August 2005).

^bOn behalf of the BABAR Collaboration.

2 Signal Identification

Searches for LFV decay in modes: $\tau \rightarrow \ell\gamma$ [1,10], $\tau \rightarrow \ell\ell\ell$ [11] and $\tau \rightarrow \ell hh$ [12] have been performed with 232.2 fb^{-1} , 91.6 fb^{-1} and 221.4 fb^{-1} of data collected by the *BABAR* experiment at $\sqrt{s} \approx 10.58 \text{ GeV}$, respectively. The characteristic feature of these decays is that both the energy and the mass of the τ -daughters are known in such an e^+e^- annihilation environment. In terms of the two independent variables: beam energy constrained mass (m_{EC}) and the energy variable $\Delta E = E_\tau - \sqrt{s}/2$, where E_τ is the energy of the τ -daughters in center-of-mass system, the signal is clustered around $(m_\tau, 0)$ in the $(m_{\text{EC}}, \Delta E)$ plane.

The identification of daughters from signal τ decays are optimized for searches for each decay mode separately. The electrons are identified from the energy deposited in the electromagnetic calorimeter and momentum of the track measured in the drift chamber with an efficiency of 91% for $\tau \rightarrow e\gamma$ and $\tau \rightarrow \ell\ell\ell$ searches. The muons are identified by its minimal ionizing particle signature in the calorimeter and hits in the instrumented flux return with an efficiency of 82%, 63% and 44% in $\tau \rightarrow \mu\gamma$, $\tau \rightarrow \ell\ell\ell$ and $\tau \rightarrow \ell hh$ searches respectively. The kaons are identified using the measured rate of ionization loss in the drift chamber and the measured Cherenkov angle in a ring-imaging detector with an efficiency of 81%. The mis-identification rates for a pion track to be identified as an electron, a muon or a kaon are 0.1%, 1.0 – 4.8%, 1.4% respectively.

3 Background estimation

The primary backgrounds are from Bhabha or di-muon events, which are restricted to a narrow band at small values of $|\Delta E|$, or the $e^+e^- \rightarrow \tau^+\tau^-$ events, which are restricted to negative values of ΔE , because the signal topology reconstruction does not account for the missing neutrino's. The remaining backgrounds from $e^+e^- \rightarrow q\bar{q}$ are uniformly distributed.

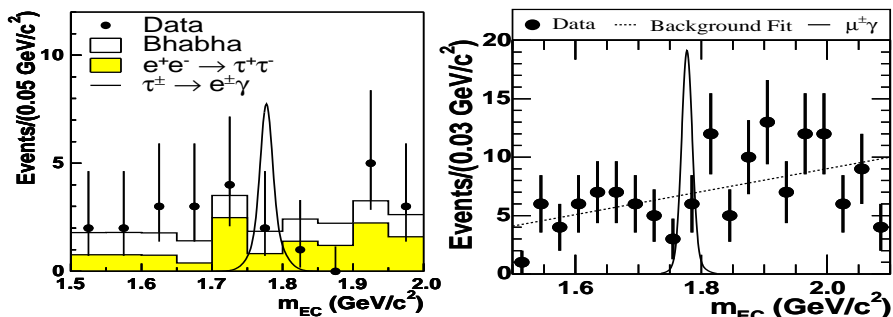


Figure 2: m_{EC} distribution inside a $\pm 2\sigma$ band in ΔE for $\tau \rightarrow \ell\gamma$ searches.

For $\tau \rightarrow \ell\gamma$ searches, the signal probability density function (PDF) is described by a double Gaussian shape in m_{EC} , and the background is well described by a constant PDF or with a small slope in m_{EC} inside a $\pm 2\sigma$ band in ΔE , as shown in Figure 2 for $\tau \rightarrow e\gamma$ (left) and $\tau \rightarrow \mu\gamma$ (right) decays.

For $\tau \rightarrow \ell\ell\ell$ (lhh) searches, the background PDF's are analytically parameterized as function of ΔE and $\Delta M = m_{daughters} - m_\tau$, where $m_{daughters}$ is the reconstructed mass of the τ daughters. The background rates are determined by un-binned maximum likelihood fits to the data, shown along with the selected signal MC events in Figure 3 and 4 for $\tau \rightarrow \ell\ell\ell$ and $\tau \rightarrow lhh$ decay modes respectively.

All these searches are performed in a blinded manner, where the background predictions from sideband data are compared to the data inside the signal region, only after the optimization and systematic studies have been completed.

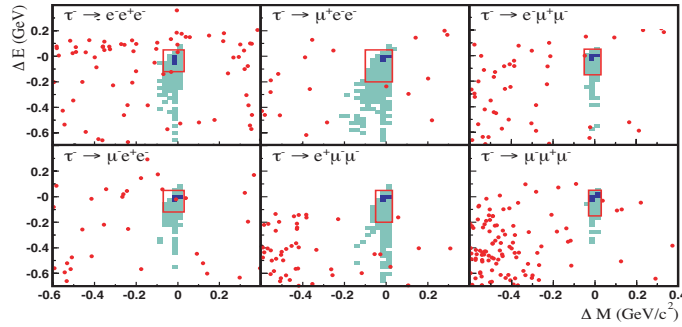


Figure 3: Observed data as dots and the boundaries of the signal region in $(\Delta M, \Delta E)$ plane for $\tau \rightarrow \ell\ell\ell$ searches. The dark and light shading indicates contours containing 50% and 90% of the selected MC signal events, respectively.

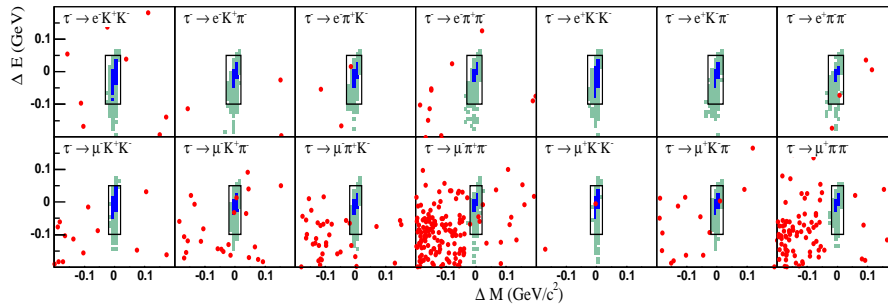


Figure 4: Observed data as dots and the boundaries of the signal region in $(\Delta M, \Delta E)$ plane for $\tau \rightarrow lhh$ searches. The dark and light shading indicates contours containing 50% and 90% of the selected MC signal events, respectively.

4 Results

No signal has been observed. Upper limits at 90% confidence level (C.L.) are set using: $\mathcal{B}_{UL}^{90} = N_{UL}^{90}/(2\varepsilon\mathcal{L}\sigma_{\tau\tau})$, where N_{UL}^{90} is the 90% C.L. upper limit on the number of signal events for N_{obs} events observed when N_{bgd} background events are expected, and ε is the signal efficiency. Efficiency estimates, the number of expected background events (N_{bgd}) in the signal region (with total uncertainties), the number of observed events (N_{obs}) in the signal region, and the 90% C.L. upper limit (\mathcal{B}_{UL}^{90}) for each decay mode are tabulated below:

Mode	Efficiency [%]	N_{bgd}	N_{obs}	$\mathcal{B}_{UL}^{90} (10^{-7})$
$e^-\gamma$	4.7 ± 0.3	1.9 ± 0.4	1	1.1
$\mu^-\gamma$	7.4 ± 0.7	6.2 ± 0.5	4	0.7
$e^-e^+e^-$	7.3 ± 0.2	1.5 ± 0.1	1	2.0
$\mu^+e^-e^-$	11.6 ± 0.4	0.4 ± 0.1	0	1.1
$\mu^-e^+e^-$	7.7 ± 0.3	0.6 ± 0.1	1	2.7
$e^+\mu^-\mu^-$	9.8 ± 0.5	0.2 ± 0.1	0	1.3
$e^-\mu^+\mu^-$	6.8 ± 0.4	0.4 ± 0.1	1	3.3
$\mu^-\mu^+\mu^-$	6.7 ± 0.5	0.3 ± 0.1	0	1.9
$e^-K^+K^-$	3.8 ± 0.2	0.2 ± 0.1	0	1.4
$e^-K^+\pi^-$	3.1 ± 0.1	0.3 ± 0.1	0	1.7
$e^-\pi^+K^-$	3.1 ± 0.1	0.1 ± 0.1	1	3.2
$e^-\pi^+\pi^-$	3.3 ± 0.2	0.8 ± 0.1	0	1.2
$\mu^-K^+K^-$	2.2 ± 0.1	0.2 ± 0.1	0	2.5
$\mu^-K^+\pi^-$	3.0 ± 0.2	1.7 ± 0.3	2	3.2
$\mu^-\pi^+K^-$	2.9 ± 0.2	1.0 ± 0.2	1	2.6
$\mu^-\pi^+\pi^-$	3.4 ± 0.2	3.0 ± 0.4	3	2.9
$e^+K^-K^-$	3.9 ± 0.2	0.0 ± 0.0	0	1.5
$e^+K^-\pi^-$	3.2 ± 0.1	0.2 ± 0.1	0	1.8
$e^+\pi^-\pi^-$	3.4 ± 0.2	0.4 ± 0.1	1	2.7
$\mu^+K^-K^-$	2.1 ± 0.1	0.1 ± 0.1	1	4.8
$\mu^+K^-\pi^-$	2.9 ± 0.2	1.5 ± 0.3	1	2.2
$\mu^+\pi^-\pi^-$	3.3 ± 0.2	1.5 ± 0.3	0	0.7

5 Summary

An improvement of five order of magnitude in the upper limits for 4 LFV τ decay modes over the past two decades is shown in Figure 5. The next five years promises to be most interesting phase in this evolution, when experimental results approach closer the predictions from different theoretical models.

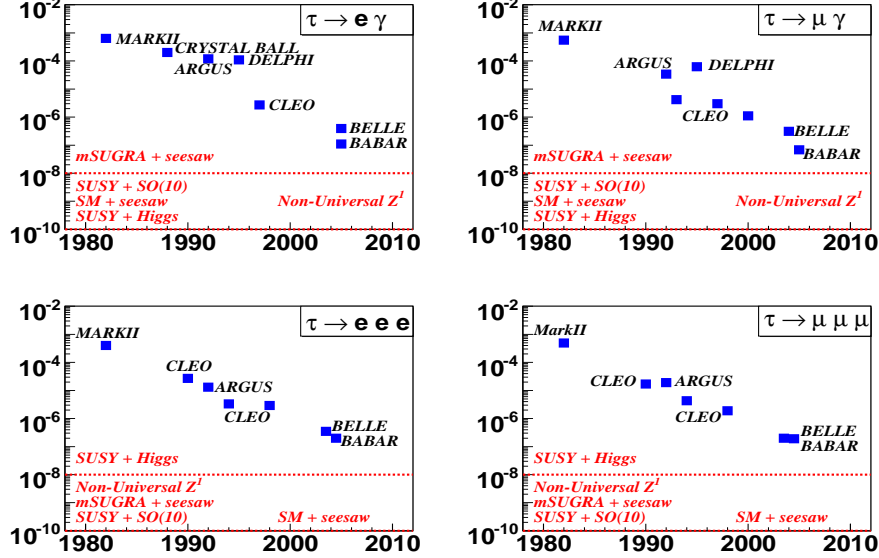


Figure 5: Evolution of experimental bounds (\mathcal{B}_{UL}^{90}) and some predictions.

References

- [1] B. Aubert *et al.* [BABAR Collaboration], Phys. Rev. Lett. **95**, 041802 (2005).
- [2] J. R. Ellis, M. E. Gomez, G. K. Leontaris, S. Lola, D. V. Nanopoulos, Eur. Phys. J. C **14**, 319 (2000).
- [3] J. R. Ellis, J. Hisano, M. Raidal, Y. Shimizu, Phys. Rev. D **66**, 115013 (2002).
- [4] A. Masiero, S. K. Vempati, O. Vives, Nucl. Phys. B **649**, 189 (2003).
- [5] T. Fukuyama, T. Kikuchi, N. Okada, Phys. Rev. D **68**, 033012 (2003).
- [6] G. Cvetič, C. Dib, C. S. Kim, J. D. Kim, Phys. Rev. D **66**, 034008 (2002) [Erratum-ibid. D **68**, 059901 (2003)].
- [7] C. x. Yue, Y. m. Zhang, L. j. Liu, Phys. Lett. B **547**, 252 (2002).
- [8] A. Dedes, J. R. Ellis, M. Raidal, Phys. Lett. B **549**, 159 (2002).
- [9] A. Brignole, A. Rossi, Phys. Lett. B **566**, 217 (2003).
- [10] B. Aubert *et al.* [BABAR Collaboration], arXiv:hep-ex/0508012. Submitted to Phys. Rev. Lett. (2005).
- [11] B. Aubert *et al.* [BABAR Collaboration], Phys. Rev. Lett. **92**, 121801 (2004).
- [12] B. Aubert *et al.* [BABAR Collaboration], Phys. Rev. Lett. **95**, 191801 (2005).